HHS Public Access

Author manuscript

J Bone Miner Res. Author manuscript; available in PMC 2020 November 29.

Published in final edited form as:

J Bone Miner Res. 2020 January ; 35(1): 143–154. doi:10.1002/jbmr.3864.

Calcium-Sensing Receptors in Chondrocytes and Osteoblasts Are Required for Callus Maturation and Fracture Healing in Mice

Zhiqiang Cheng, **Alfred Li**, **Chia-Ling Tu**, **Christian Santa Maria**, **Nicholas Szeto**, **Amanda Herberger**, **Tsui-Hua Chen**, **Fuqing Song**, **Jiali Wang**, **Xiaodong Liu**, **Dolores M Shoback**, **Wenhan Chang**

Endocrine Research Unit, Department of Veterans Affairs Medical Center, NCIRE, University of California, San Francisco, CA, USA

Abstract

Calcium and its putative receptor (CaSR) control skeletal development by pacing chondrocyte differentiation and mediating osteoblast (OB) function during endochondral bone formation—an essential process recapitulated during fracture repair. Here, we delineated the role of the CaSR in mediating transition of callus chondrocytes into the OB lineage and subsequent bone formation at fracture sites and explored targeting CaSRs pharmacologically to enhance fracture repair. In chondrocytes cultured from soft calluses at a closed, unfixed fracture site, extracellular [Ca^{2+}] and the allosteric CaSR agonist (NPS-R568) promoted terminal differentiation of resident cells and the attainment of an osteoblastic phenotype. Knockout (KO) of the *Casr* gene in chondrocytes lengthened the chondrogenic phase of fracture repair by increasing cell proliferation in soft calluses but retarded subsequent osteogenic activity in hard calluses. Tracing growth plate (GP) and callus chondrocytes that express Rosa26-tdTomato showed reduced chondrocyte transition into OBs (by >80%) in the spongiosa of the metaphysis and in hard calluses. In addition, KO of the *Casr* gene specifically in mature OBs suppressed osteogenic activity and mineralizing function in bony calluses. Importantly, in experiments using PTH (1–34) to enhance fracture healing, co-injection of NPS-R568 not only normalized the hypercalcemic side effects of intermittent PTH (1–34) treatment in mice but also produced synergistic osteoanabolic effects in calluses. These data indicate a functional role of CaSR in mediating chondrogenesis and osteogenesis in the fracture callus and the potential of CaSR agonism to facilitate fracture repair.

Keywords

CARTILAGE; CaSR KNOCKOUT; CHONDROCYTE; CHONDROGENESIS; ENDOCHONDRAL BONE FORMATION; FRACTURE HEALING; OSTEOBLAST; OSTEOGENESIS; UNFIXED FRACTURE

Address correspondence to: Wenhan Chang, PhD, Endocrine Unit (111N), VAMC 4150 Clement Street, San Francisco, CA 94158, USA. wenhan.chang@ucsf.edu.

Authors' roles: All authors contributed, read, and approved this manuscript. ZC, AL, CSM, CLT, DMS, and WC designed the study. ZC, AL, CSM, NS, AH, THC, FS JW, XL, CLT, and WC conducted the study. ZC, AL, CSM, THC, CLT, and WC collected data. ZC, AL, CSM, NS, THC, CLT, DMS, and WC performed data analysis and interpretation: ZC, AL, DMS, and WC wrote the manuscript with support of CLT. WC takes responsibility for the integrity of the data analysis.

Disclosures

All authors state that they have no conflicts of interest.

Introduction

Both osteoporotic and traumatic fractures are complicated by high rates (10% to 20%) of impaired healing that present as delayed union or nonunion. Delayed healing and nonunion of fractures greatly impact the quality of life of patients and particularly impairs rehabilitation of elderly patients.[1,2] Daily or "intermittent" PTH (1–34) therapy, approved by the FDA to treat severe osteoporosis, has modest beneficial effects on fracture repair in small clinical trials.[3,4] Hypercalcemic effects of PTH (1–34), however, deter its use at higher doses than those clinically approved for osteoporosis and thus limit the potential of using such doses to promote fracture healing.[5,6] New strategies targeting other molecules and/or enhancing the anabolic effects of PTH (1–34) are needed to improve fracture repair.

Endochondral bone formation controls longitudinal bone growth from early embryonic stages to adolescence.[7] This process is initiated by the condensation of mesenchymal progenitor cells, which differentiate into chondrocytes.[7] Committed chondrocytes progress sequentially through stages of proliferation, maturation, hypertrophy, and terminal differentiation in columns of cells within the growth plate (GP) before the terminally differentiated chondrocytes transition into the osteoblastic lineage to form bone in spongiosa and other bone sites.[8–10] Chondrocytes in the soft callus, particularly in unfixed fractures, recapitulate key steps of endochondral cell differentiation, including chondrocyte-to-osteoblast (OB) transition,[11,12] at early stages of fracture repair. At the later stages, osteogenic and osteoclastic activities take over to bridge and remodel the disrupted bony elements, returning them to the prior normal shape and strength. However, cartilage within a callus has a transient existence (days to weeks), whereas GPs function for years until long bone growth ceases. In addition to endochondral bone formation, "membranous bone formation" also critically mediates bone repair, particularly in fixed fractures, through actions of osteoprogenitors/osteoblasts derived from periosteum,[13] muscle,[13–15] pericyte,[16] bone marrow[17–19] and commit to osteogenic lineage directly without transition through chondrogenic phase.

Ca^{2+} is critical for bone health and normal fracture repair by serving as an essential substrate of mineralized bone matrix and a primary extracellular signal driving chondrocyte and OB differentiation.[20] The extracellular calcium-sensing receptor (CaSR), a member of the family C of the G-protein coupled receptor (GPCR) superfamily, renders cells able to respond to subtle physiological changes in extracellular $[Ca^{2+}]$ ($[Ca^{2+}]_e$) in diverse tissues (eg, parathyroid glands, kidneys, and bone).[21,22] In the GP, the CaSR first appears in maturing chondrocytes, and its expression increases as chondrocytes approach terminal differentiation.[23] Cultures of primary GP chondrocytes (GPCs)[24] and rat chondrogenic RCJ3.1.C5.18 cells[25,26] recapitulate the time-dependent sequences of chondrocyte differentiation as seen in the GP. In these cultures, raising $[Ca^{2+}]_e$ in the physiological range accelerates the pace of cell terminal differentiation and promotes mineralizing function of the cells. Ablation of the CaSR specifically in chondrocytes during embryonic or postnatal development in mice delays chondrocyte terminal differentiation, impedes cartilage mineralization, and retards bone growth,[20] supporting a nonredundant role of the CaSR in cartilage development. Furthermore, CaSRs are abundantly expressed in mature OBs and osteocytes. Selective ablation of CaSR in OBs in vivo reduced OB/osteocyte survival and

differentiation, decreased skeletal mineralization, and retarded bone growth, leading to multiple unhealed fractures.[20,27] Based on these observations, we hypothesize that chondrocyte CaSRs mediate transition of chondrocytes into OBs and render this source of OBs responsive to changes in Ca^{2+} availability to regulate skeletal metabolism.

The current study utilized callus chondrocyte cultures, a well-controlled tibial midshaft fracture model, chondrocyte-specific and OB-specific CaSR KO mice, and cell-tracing techniques to define the actions of CaSR in mediating chondrogenic and osteogenic activities during fracture repair. We also tested the potential of a CaSR agonist in enhancing fracture healing. These translational animal studies aim to facilitate future development of novel pharmacological regimens to promote fracture repair in patients by targeting the CaSR.

Materials and Methods

Mice

Floxed-CaSR ($CaSR^{flox/flox}$) mice[20] were bred with Cart-$CreER^T$ mice,[28] which carry a tamoxifen (Tam)-inducible $CreER^T$ transgene under the control of *Col2a1* gene promoter for chondrocyte-specific expression, to produce $^{Tam\text{-}Cart}CaSR^{flox/flox}$ mice that developed normally in the absence of Tam.[28] $^{Tam\text{-}Cart}CaSR^{flox/flox}$ mice were injected daily with Tam (2 mg/25 g body weight, in corn oil [Millipore Sigma, Burlington, MA, USA; #C8267]) through the intraperitoneal (IP) route according to specified schedules (Supplemental Fig. SS1A, Schedule #1) to induce *Casr* gene KO in the resulting $^{Tam\text{-}Cart}CaSR^{\Delta flox/\Delta flox}$ mice. $CaSR^{flox/flox}$ mice without expression of Cart-$CreER^T$ transgene were injected with Tam to serve as controls. For cell tracing experiments, $^{Tam\text{-}Cart}CaSR^{flox/flox}$ mice were bred with tdTomato mice (Jackson Laboratory, Bar Harbor, ME, USA; stock no. 007905),[29] which carry the Cre/loxP-inducible Rosa-CAG-LSL-tdTomato reporter, to mark the cells after the induction of CreER activity by Tam injections (Supplemental Fig. SS1A, schedule #2). Cart-$CreER^T$ mice without floxed-CaSR alleles were bred with Rosa-tdTomato mice to produce $^{Tam\text{-}Cart}$Rosa-tdTomato mice to serve as controls in these cell-tracing experiments. Additional controls, in which $^{Tam\text{-}Cart}$Rosa-tdTomato mice were injected with corn oil only, were performed to confirm the absence of promoter leakage without Tam, as indicted by the lack of tdTomato signals in the GP and soft calluses of the mice (data not shown). To delete CaSRs in mature OBs, $CaSR^{flox/flox}$ mice were bred with the osteocalcin (OCN)-Cre line[30] to generate $^{OCN}CaSR^{\Delta flox/\Delta flox}$ and control littermates. All mutant mice were in C57/B6 background. Mouse genotypes were determined by PCR analyses of genomic DNAs from tail snips with primer sets for the *Cre* transgene, the loxP sequence flanking the exon 7 of *Casr* gene, Rosa-CAG-LSL-tdTomato alleles (Supplemental Table SS1). Genomic DNA from callus cartilage, bone (tibial midshaft without marrow), and various tissues of the $^{Tam\text{-}Cart}CaSR^{\Delta flox/\Delta flox}$ mice and/or $CaSR^{flox/flox}$ littermates were used to confirm tissue-specific excision of the exon 7 of the *Casr* gene (Supplemental Fig. SS1B).

To test the impact of PTH (1–34) (Bachem, Torrance, CA, USA; Cat# H-5460) and/or R568 (Tocris, Minneapolis, MN, USA; Cat# 3815) on fracture healing, 3-month-old male C57/B6 mice were ear-tagged for identification, randomly assigned to groups, and injected daily with the drugs individually or in combination with specified doses for 4 weeks starting

immediately after fracture. All mice were kept in a climate-controlled room (22°C; 45% to 54% relative humidity) with a 12-hour light/12-hour dark cycle. Water and standard chow (1.3% calcium and 1.03% phosphate) were given *ad libitum*. All experiments are performed on 3-month-old adult male mice to avoid 1) pre- and perinatal developmental defects due to early ablation of *Casr* gene[20] and 2) female-specific side-effects of Tam on hormonal and reproductive systems, which could complicate data interpretation and prevent a definitive conclusion from our study. All animal experiments (Protocol #18–013) were approved and performed according to guidelines of the Institutional Animal Care and Use Committee at the San Francisco Department of Veterans Affairs Medical Center.

Tibial midshaft fracture

In the 3-month-old male $^{\text{Tam-Cart}}\text{CaSR}^{\text{flox/flox}}$, $\text{CaSR}^{\text{flox/flox, Tam-Cart-}}\text{CaSR}^{\text{flox/flox}}$// tdTomato, $^{\text{Tam-Cart}}$tdTomato, and $^{\text{OCN}}\text{CaSR}^{\Delta\text{flox}/\Delta\text{flox}}$ mice with or without 5 to 9 daily intraperitoneal (IP) injections of Tam, closed unfixed bone fractures were created unilaterally in the right mid-tibia on the second day of Tam administration (Supplemental Fig. SS1A) by 3-point bending using a Bose Electroforce 3200 Material Testing System (Supplemental Fig. S2A)[31] under general anesthesia with locally injected analgesics. The downward middle test probe, positioned exactly at the midshaft position, was controlled by an automated actuator, which retrieved the test probe immediately after the bone was fractured (as detected by an accelerated downward probe movement) to minimize soft tissue damage. X-ray radiography was performed immediately after the procedure to ensure fracture consistency (Supplemental Fig. S2B). Mice with inadequate fractures were excluded from the analyses. The mice were allowed to ambulate freely in their cages after successful fracture. Fracture calluses were collected and analyzed at times specified (Supplemental Fig. SS1A) by investigators who were blinded to mouse groupings.

Power analyses

The numbers of mice needed for the proposed μCT imaging, histomorphometric, histological, and biochemical analyses (see below sections) were determined using statistical methods of experimental design with a statistical software (DSS Research, Fort Worth, TX, USA). Per standard scientific practice, experiments were designed using alpha = 0.05 to find effects that are significant at the 95% confidence level. Using expected means and standard deviations derived from our previous studies[31] and an estimated power (1-β) of 80%, the sample sizes required to detect a difference in μCT, static, and dynamic skeletal parameters were estimated to be 8 mice/group for comparisons between KO versus Cont mice and 15 mice/group for comparisons among mice treated with or without PTH and/or R568. We added additional 20% of the estimated animal numbers to account for unsuccessful fracture or poor animal ambulation. Because of limited quantity of cartilage from each fracture site, for cell culture experiments described in Fig. 1, {FIG1} a large number of mice were used to harvest sufficient chondrocytes.

Culturing callus chondrocytes

Cartilage in the calluses at day 10 post-fracture was dissected free from surrounding fibrous tissues and preexisting cortical bones were pulled away to separate them from the cartilage. If necessary, remaining minute bony tissues were further scraped off using a 15C-type

surgical blade (Southern Anesthesia and Surgical, Inc., West Columbia, SC, USA) under a stereomicroscope. Some dissected cartilage was randomly selected for combined Alcian green (AG) and Alizarin red (AR) staining to check for inclusion of bony tissue. The rest of cartilage was then minced into small fragments and incubated briefly (15 minutes) with trypsin to remove loosely attached fibroblasts and/or OBs before the cartilage fragments were subjected to serial digestions with a mixture of collagenase IA, hyaluronidase, and deoxyribonuclease II (30 minutes per digestion with refreshed enzyme mixture) and the digested chondrocytes were collected by centrifugations. These procedures were repeated until all chondrocytes were released. We discarded the first digestion mixture as a precaution to further exclude any residual fibroblasts and OBs. This protocol produced highly enriched chondrocyte preparations, as indicated by robust expression of chondrogenic markers and strong propensity of the cells to synthesize proteoglycans-rich cartilage matrix.[24,32] The isolated callus chondrocytes were plated in monolayer at a density of 10^5 cell/cm^2 as described previously.[24–26,32,33] The cells were cultured to confluency (≈4 days) before treatments with various [Ca^{2+}] (0.5, 1.5, and 3.0 mM) with or without addition of 5 μM NPS-R568 (in 0.1% DMSO), an allosteric CaSR agonist, for 7 days. Cells were stained sequentially with von Kossa (VK) and AG reagents for Ca^{2+}-containing mineral and proteoglycans, respectively, or used for RNA analyses as previously described.[24,32]

Micro-computed tomography (μCT) and histomorphometric analyses

Fracture calluses and nonfractured tibias were dissected free of attached muscle at days 10 and 28 post-fracture, fixed in 10% phosphate-buffered formaldehyde (PBF), and stored in 70% ethanol. Because of poor delineation between cartilage versus immature bone mineral by μCT in the 10-day-old calluses, only 28-day fracture calluses were analyzed using the Scanco μCT 50 scanner (Scanco Medical AG, Basserdorf, Switzerland) with 10 μm voxel size and X-ray energies of 55 kVp and 109 μA. A lower excluding threshold of 400 mg hydroxyapatite (HA)/mm^3 was applied to segment total mineralized bone matrix from soft tissue in studies of control and KO mice, and a high threshold of 1000 mg hydroxyapatite (HA)/mm^3 was further used to segment bone with high-density mineral from those with low-density mineral in studies of mice treated with PTH and/or R568. Linear attenuation was calibrated using a Scanco hydroxyapatite phantom. The regions of interest (ROI) included the entire callus without existing cortical clearly distinguished by its anatomical location and much higher mineral density. For trabecular bone parameters in nonfractured tibias, the ROI included all trabecular bone within 1 mm below the growth plate. μCT reconstruction and quantitative analyses were performed to obtain the following structural parameters with slightly modified acronyms to indicate their trabecular (Tb) versus callus (Cal) origin: total Tb or callus volume (Tb.TV or Cal.TV); Tb or callus bone volume (Tb.BV or Cal.BV), which excludes the preexisting bone; Tb.BV/TV or Cal.BV/TV ratio; thickness (Tb.Th or Cal.Th); number (Tb.N or Cal.N); connectivity density (Tb.CD or Cal.CD); and spacing (Tb. Sp or Cal.Sp).

After μCT scanning, both 10- and 28-day fractured bones were dehydrated with 100% ethanol, defatted with xylene, and embedded in methyl methacrylate (MMA) (Sigma, St. Louis, MO, USA). Serial sections (5 or 10 μm in thickness) were cut and mounted on gelatin-coated slides for different staining procedures. Adjacent sections (≈50 to 100 μm

apart) from each side of the centermost (usually the largest) section of each callus were stained with 1) combined VK/Safranin O (SO); 2) Goldner; or 3) tartrate-resistant acid phosphatase (TRAP) reagent to assess static histomorphometric parameters. Averaged number of the 2 callus sections from each of the fractured bones was used for statistical analyses. To assess dynamic bone parameters, calcein and demeclocycline (15 mg/kg body weight) were injected intraperitoneally 3 days and 1 day before bone collection. This shorter interval between calcein and demeclocycline injections, in contrast to the conventional 7/3-day regimen for normal remodeling activities,[34] was adapted because it is proven to be more accurate in detecting faster bone remodeling activity during fracture repair in preliminary experiments (data not shown). The terminology and units used for histomorphometric parameters are those recommended by the Histomorphometry Nomenclature Committee of the American Society for Bone and Mineral Research,[35] except that trabecular bone (Tb) was replaced with callus bone (Cal). In addition, callus cartilage volume (Cal.CV), which stains positively only for SO, and mineralized cartilage volume (MCV), which stains positively for both SO and VK, were also assessed in soft calluses at day 10 post-fracture. Images were acquired by a Zeiss AXIO Imager M1 Microscope and analyzed by Bioquant OSTEO 2009 software (Bioquant, Nashville, TN, USA).

Cell tracing

For cell tracing experiments, both fractured and nonfractured bones were collected from $^{\text{Tam-Cart}}\text{CaSR}^{\text{flox/flox}}$//tdTomato (KO) and $^{\text{Tam-Cart}}$ tdTomato (control) mice at day 8 post-fracture, when most of the soft callus was largely composed of cartilage, and at day 21 post-fracture, when soft callus was just completely converted to bony callus. After fixation in 4% PFA and decalcification in 10% EDTA (pH 7.0) for 14 days, the bones were embedded in OCT media and sectioned in 7 μm thickness. Two adjacent sections (≈70 μm apart) from each side of the centermost section of each callus were mounted/counterstained with a medium containing DAPI (art no. DUO82040–5ML, Sigma). Red tdTomato and blue DAPI fluorescent images were obtained and analyzed by TissueGnosticts HistoQuest software (TissueGnosticts, USA, Ltd, Tarzana, CA, USA). The averages of 2 callus sections from each of the fractured bones and of the 2 growth plate sections from each of the contralateral nonfractured bones were used for statistical analyses.

Quantitative real-time polymerase chain reaction (qPCR) assays

Total RNA was extracted from cartilage dissected from 10-day soft calluses, cultured callus chondrocytes, or 28-day bony callus without preexisting cortical bone. For soft callus, the majority of preexisting cortical bone could be easily pulled out, followed by microdissection to remove any remaining bone fragments, which were easily distinguished by their white opaque color and hard texture. For the bony callus, microdissection was performed to separate (cut or scrape off) “trabeculae-like” bony callus from the preexisting cortex. Real-time PCR analyses were performed using murine specific Taqman primers/probes sets for aggrecan (AGG), alpha-subunits of type II [Col(II)] or type X [Col(X)] collagen, osteopontin (OPN), osteonectin (ON), osteocalcin (OCN), dentin matrix protein 1 (DMP1), insulin-like growth factor 1 (IGF1) and its receptor (IGF1R), and parathyroid hormone-

related peptide (PTHrP), as reported previously.[20,27] Levels of gene expression were normalized to the level of housekeeping gene ribosomal protein L_{19}.

Serum chemistries

Blood was drawn from mice 3 hours after the last injection of PTH (1–34) and/or R568 or vehicle by the retroorbital route under anesthesia by isoflurane inhalation. Serum samples were prepared by centrifugation and analyzed for total serum calcium and phosphate (Pi) by an automated ACE Alera Clinical Chemistry bioanalyzer (Alfa Wassermann, Inc, West Caldwell, NJ, USA).

Statistics

Comparisons were evaluated by unpaired two-tailed Student's *t* tests between KO and controls or by one-way or two-way ANOVA followed by Tukey's test for multiple comparisons using Prism 8 for MacOS software (GraphPad Software, Inc., San Diego, CA, USA). Values are expressed as mean ± SEM. Any p values <0.05 were considered significant for all analyses.

Results

CaSR expression and actions in callus chondrocytes

To delineate the actions of the CaSR during the chondrogenic phase of fracture repair, we employed a closed, unfixed fracture model produced by unilateral controlled 3-point bending at the midshaft of right tibia of the mouse[31] (Supplemental Fig. S2A). This procedure produces relatively consistent fractures, due to its precise location and minimal soft tissue damage. This unfixed fracture also produced prolonged chondrogenic activity (compared with fixed fracture models) from days 6 to 14 post-fracture in mice, followed by osteogenic activity until complete bridging of the fractured bone was evident at day 28 (Supplemental Fig. S2B) and then by active bone remodeling until completion of the repair. We first confirmed the expression of CaSR protein by immunohistochemistry using a custom-made polyclonal antibody against the ADDYGRPGIEKFREEAEE epitope in the extracellular domain of the CaSR[36] (Supplemental Fig. SS1C, Cont) and the expression of RNA by quantitative qPCR (Fig. 2C, leftmost panel, CaSR:Cont) in chondrocytes from soft calluses of mice 10 days after fracture.

To determine whether these CaSRs are functional, we carefully dissected callus cartilage free of bone tissues (Fig. 1A), enzymatically released chondrocytes, and grew the cells in 2D culture to test their responses to changes in extracellular $[Ca^{2+}]$ ($[Ca^{2+}]_e$) (Fig. 1B, C) and the allosteric CaSR agonist (NPS-R568) (Fig. 1D, E). These cells grew to confluence after ≈4 days of plating (10^5 cells/cm^2) in monolayer and continued to proliferate, forming multilayer sheets/nodules (Fig. 1B, D) as seen in cultures of primary GP chondrocytes[24,32] and clonal nontransformed rat chondrogenic RCJ.3.1.C518 cells.[25,26] Our previous studies of the latter two cell cultures consistently showed spontaneous cell progression through the steps of endochondral differentiation (at 1.8 mM Ca^{2+}) as seen in the GP in vivo in a time-dependent manner and the ability of raising $[Ca^{2+}]_e$ over a wide physiological range (0.5 to 3 mM) to alter the pace of cell differentiation.[24–26,32,33] Compatible with the responses

from cultures of GP chondrocytes and RCJ3.1C5.18 cells, raising $[Ca^{2+}]_e$ from 0.5 to 1.5 and 3.0 mM dose-dependently altered chondrogenic activity of callus chondrocytes. After culture at 0.5 mM Ca^{2+} for 7 days (a total of 11 days), we observed a relatively uniform proteoglycan-rich (AG-positive) cartilage matrix with a very high expression ratio (400:1) of the chondrocyte marker, α1 subunit of type II collagen [α_1(II)], over the mature osteoblastic marker (OCN), indicating a highly enriched chondrocyte culture. In contrast, growth of these cultures at 3 mM Ca^{2+} for 7 days produced a 15-fold increase in the expression of OCN and 10-fold and 22-fold decreases in the expression of α_1(II) and Agg, respectively, compared with the cultures at 0.5 mM Ca^{2+}, suggesting a profound Ca^{2+}-dependent transition of cellular phenotype from chondrogenic to osteogenic. The latter cell transition was further indicated by a global reduction of AG staining and an increase in Ca^{2+}-containing mineral in cultures at high Ca^{2+}. These effects of high $[Ca^{2+}]_e$ on chondrocyte differentiation and their putative transition into an “osteoblast-like” phenotype could be facilitated by adding NPS-R568 (or R568), which enhances the sensitivity of the CaSR, to cultures at low $[Ca^{2+}]_e$ (Fig. 1D, E), supporting the action of CaSR agonism in mediating differentiation of callus chondrocytes.

Delayed chondrocyte differentiation and fracture repair in mice lacking chondrocyte CaSRs

To further define the actions of the CaSR in callus chondrocytes in vivo, we studied the impact of acute chondrocyte-specific *Casr* gene KO on chondrogenic and osteogenic activities in calluses at different times of repair by employing a Tam-inducible, chondrocyte-targeted CaSR KO ($^{Tam\text{-}Cart}CaSR^{\Delta flox/\Delta flox}$, KO) mouse model. Gene KO in the latter model was induced by giving 5–9 consecutive daily injections of Tam to $^{Tam\text{-}Cart}CaSR^{flox/flox}$ mice, which carry the inducible chondrocyte-specific $CreER^T$ ($^{Tam\text{-}Cart}CreER^T$) alleles[28] and homozygous floxed-CaSR alleles,[20] 1 day before fracture (Supplemental Fig. SS1A). The ability of Tam to ablate CaSR gene, protein, and RNA expression in $^{Tam\text{-}Cart}CaSR^{\Delta flox/\Delta flox}$ callus chondrocytes was confirmed, respectively, by genomic DNA (Supplemental Fig. SS1B), immunohistochemical (Supplemental Fig. S1C), and RNA (Fig. 2C) analyses.

As assessed by histomorphometry at day 10 post-fracture, the callus sizes (Cal.TV) of $^{Tam\text{-}Cart}CaSR^{\Delta flox/\Delta flox}$ mice were ≈50% larger compared with those from $CaSR^{flox/flox}$ control (Cont) littermates, which also received Tam (Fig. 2A, B). {FIG2} This size change was accompanied by an increased callus cartilage fraction (Cal.CV/TV), which was stained positively by Safranin O (SO) reagents (Fig. 2A, B), and reduced callus trabecula-like bone fraction (Cal.BV/TV), which was demonstrated by VK reagents with preexisting cortical bone excluded from the quantitation. This reduced Cal.BV/TV was mainly due to decreases in callus bone thickness (Cal.Th) and number (Cal.N) and an increase in spacing (Cal.Sp) (Fig. 2B). Despite the increased Cal.CV/TV, the fraction of mineralized cartilage (Cal.MCV/CV), which was made by terminally differentiated chondrocytes and stained positively by both SO and VK reagents, was reduced by ≈50% in the KO versus Cont calluses (Fig. 2A, B). Goldner staining of adjacent callus sections showed profound reductions in newly synthesized osteoid in the chondrocyte-to-OB transition zone of the KO versus Cont mice (Supplemental Fig. S3), indicating defects in osteogenic activity. Consistent with these morphological changes were increased RNA expression of chondrogenic markers, α_1-

subunits of type II [α_1(II)] and X collagen [α_1(X)], and reduced expression of the terminal differentiation marker, osteopontin (OPN), and the mature OB marker, osteocalcin (OCN), in calluses dissected free of preexisting cortical bone (Fig. 2C).

As we have shown previously, there is a reduced ability of high $[Ca^{2+}]_e$ to promote terminal differentiation and matrix mineralization of cultured GPCs lacking IGF1R.[20] We, therefore, assessed if CaSR KO impeded terminal differentiation by interfering with this signaling pathway. In support of this hypothesis, we observed significantly decreased expression of IGF1 and IGF1R RNA in the soft callus of $^{\text{Tam-Cart}}\text{CaSR}^{\Delta\text{flox}/\Delta\text{flox}}$ (KO) versus Cont mice (Fig. 2C). We have also shown that Ca^{2+}/CaSR signaling antagonizes the proliferative actions of PTHrP/PTH1R signaling to promote chondrocyte terminal differentiation.[24] To determine whether the enlarged callus cartilage in the CaSR KO mice was due to increased PTHrP expression (which might lead to increased cell proliferation), we assessed PTHrP RNA expression and performed immunohistochemical detection of proliferating cell nuclear antigen (PCNA) and terminal deoxynucleotidyl transferase dUTP nick end labeling (TUNEL) assays to determine the status of proliferation and apoptosis in these calluses. There were robust increases in PTHrP RNA expression (≈3-fold) (Fig. 2C) and in the number of PCNA (+) cells (≈2-fold) (Fig. 2D), along with no changes in the number of TUNEL(+) cells (Fig. 2E) in the KO versus Cont calluses. The increased cell proliferation also led to an increase in overall cell density in the callus cartilage of the KO versus Cont mice (Fig. 2F). These findings suggested that enhanced PTHrP signaling, in the absence of CaSR expression, could be responsible for the enlargement of cartilage by promoting cell proliferation. These and the above morphological and biochemical data together indicate a critical role for CaSRs in promoting chondrocyte terminal differentiation, transition of cartilage to bone, and mineralization in callus cartilage.

To examine whether the aforementioned chondrogenic defects interfered with subsequent osteogenic activities, we assessed static and dynamic bone structural parameters in calluses at day 28 post-fracture, when chondrogenic activities had ceased for several days in our fracture model. μCT analyses showed significantly thinner and demineralized calluses in the $^{\text{Tam-Cart}}\text{CaSR}^{\Delta\text{flox}/\Delta\text{flox}}$ (KO) versus Cont mice, as indicated by reduced Cal.BV/TV and Cal.Th and increased Cal.Sp (Fig. 3A). {FIG3} Similar reductions in Tb.BV/TV and Tb.Th and increases in Tb.Sp were observed in the secondary spongiosa in the proximal tibias of contralateral bones of $^{\text{Tam-Cart}}\text{CaSR}^{\Delta\text{flox}/\Delta\text{flox}}$ (KO) versus Cont mice (Fig. 3B), indicating an osteogenic defect in response to the ablation of CaSR in GP chondrocytes of nonfractured bone. The changes in callus bone parameters in the KO mice were confirmed by histomorphometric analyses of callus sections stained with SO and VK reagents (Fig. 3C). In addition, the latter analysis showed a significant decrease in callus bone number (Cal.N). Furthermore, the bony calluses of KO mice displayed larger amounts of unmineralized osteoid (Fig. 3D, in pink) by Goldner staining and reductions in mineralizing surface and bone formation rate assessed by dual calcein and demeclocycline labeling (Fig. 3E), when compared with Cont mice. These data indicate overall reductions in osteogenic activity and mineralizing function in the metaphysis and calluses of mice lacking chondrocyte CaSRs. Analyses of osteoclast number and erosion surfaces in TRAP-stained callus sections showed comparable osteoclastic activity between the two groups (Fig. 3F), suggesting that defects in

OB function are the major cause for the poorly developed bony callus in $^{\text{Tam-Cart}}\text{CaSR}^{\Delta\text{flox}/\Delta\text{flox}}$ mice.

Delayed transition of CaSR-deficient chondrocytes into osteoblastic lineage cells in fracture calluses

We hypothesized that delayed maturation/terminal differentiation of callus chondrocytes lacking CaSRs impaired their ability to transition into the osteoblastic lineage, consequently reducing osteogenic activity in the subsequent bony calluses. To test this hypothesis, we bred $^{\text{Tam-Cart}}\text{CaSR}^{\text{flox}/\text{flox}}$ mice or $^{\text{Tam-Cart}}\text{CreER}^{\text{T}}$ mice with mice carrying a floxed Rosa-CAG-LSL-tdTomato gene allele[29] to introduce red tdTomato fluorescent protein in chondrocytes in the presence or absence of Tam-induced CaSR KO, respectively. Daily injections of Tam until day 8 post-fracture activated tdTomato expression in nearly all chondrocytes in the soft callus of both CaSR KO and Cont mice (Fig. 4A; {FIG4} Soft Callus). Similarly, ≈60% of GPCs in the metaphysis of nonfractured bones in both KO and Cont groups expressed tdTomato, with no significant difference between the two groups (Fig. 4A; Metaphysis, GP). However, we observed significantly ($p < 0.01$) higher numbers of tdTomato(+) OBs on the surface of bone in the primary (1°) and secondary (2°) spongiosa of Cont mice, when compared with that in KO mice (Fig. 4A; Metaphysis, areas below GP). Similarly, at day 21 post-fracture, when chondrogenic activities in fracture calluses had ceased for several days, we observed significantly higher numbers of tdTomato(+) OBs in both bony calluses and spongiosa of Cont mice, when compared with KO mice (Fig. 4B). Interestingly, numbers of tdTomato(+) chondrocytes were also reduced in the tibial GPs of the KO mice at day 28 post-fracture (Fig. 4B). To further examine whether those tdTomato(+) cells can differentiate into mature OBs, we performed immunohistochemistry with antisera against a mature OB marker (OCN). We observed ≈60% of tdTomato(+) cells, which were also positive for OCN expression, in the 1° and 2° spongiosa and ≈40% of double positive cells in bony callus of the control mice (Fig. 4C). Interestingly, at both anatomical sites, the % of double tdTomato(+);OCN(+) cells were significantly lower (≈40 and ≈25%, respectively) in the mice with CaSR KO (Fig. 4, scatter plots), supporting a role of CaSR in mediating maturation of OB into the state that expresses OCN. Our study also revealed substantial amounts of tdTomato (+)/OCN(−) cells with unknown identities at those sites. The latter cells could represent immature cells transitioning to mature OBs or cells committing to other cell lineages. Future studies are required to distinguish these possibilities. Nevertheless, the above data together indicate a deficient chondrocyte-to-OB transition in GPs and fracture calluses in the absence of chondrocyte CaSRs.

CaSRs mediate osteogenic activities in bony callus

To test whether the impaired osteogenic activity and mineralizing function in bony calluses of $^{\text{Tam-Cart}}\text{CaSR}^{\Delta\text{flox}/\Delta\text{flox}}$ mice lacking chondrocyte CaSRs (Fig. 3) were at least in part due to the continuous absence of CaSR function in the chondrocyte-derived OBs, we studied the effects of CaSR KO targeted specifically to mature OBs. We bred OCN promoter-driven Cre (OCN-Cre) line[30] with the floxed-CaSR mice and studied the resulting $^{\text{OCN}}\text{CaSR}^{\Delta\text{flox}/\Delta\text{flox}}$ and control littermates by histomorphometric analyses. We reported previously that the $^{\text{OCN}}\text{CaSR}^{\Delta\text{flox}/\Delta\text{flox}}$ mice developed normally but displayed osteopenic trabeculae in their long bones at 3 months of age.[20] Similarly, at day 28 post-fracture, we observed osteopenic

calluses, reflected in reduced Cal.BV/TV and Cal.N and increased Cal.Sp (Fig. 5A), {FIG5} along with reduced mineralizing surface and bone formation rates (Fig. 5B) and decreased expression osteoblastic markers (Fig. 5C) in the $^{OCN}CaSR^{\Delta flox/\Delta flox}$ versus control mice. These data support an important role of OB CaSRs in normal fracture repair.

A novel regimen for skeletal anabolism in fracture calluses by targeting CaSRs

Given the above anabolic actions of CaSRs in callus chondrocytes and OBs, we examined the potential for targeting the CaSR to enhance fracture repair. We first tested the effects of an injectable allosteric CaSR agonist (or calcimimetic), NPS-R568, on serum calcium and phosphorus, as calcimimetics such as cinacalcet are used to treat patients with hypercalcemia and both primary and secondary hyperparathyroidism (HPTH).[37] In mice injected once daily with R568 for 4 weeks, this compound did lower serum calcium and phosphate acutely by 3 hours after (Fig. 6A), {FIG6} raising a concern for using this compound alone to enhance fracture healing. Considering that the acute hypocalcemic effect of R568 parallels the opposite acute hypercalcemic effects of PTH (1–34) (Fig. 6A), we hypothesized that combining PTH and R568 could mutually offset their effects on serum calcium and concomitantly produce synergistic skeletal anabolism in fracture calluses. Indeed, co-injections of R568 (20 μmol/kg/d) prevented the acute rise in serum [Ca^{2+}] in 3-month-old male mice subjected to daily injections of PTH (1–34) up to 40 μg/kg (Fig. 6A). Likewise, co-injections of 40 μg/kg PTH (1–34) completely abrogated the acute hypocalcemia seen in the mice 3 hours after injection of R568 alone (Fig. 6A). Interestingly, R568 co-injected with lower doses of PTH (1–34) (10 and 20 μg/kg) actually produced acute mild hyperphosphatemia along with mild hypocalcemia. However, these hyperphosphatemic effects disappeared with the 40 μg/kg PTH (1–34) dose, at which the hypocalcemic effects of R568 (20 μmole/kg) were also completely offset. It appears that the R568 induced opposite effects on phosphate metabolism in the presence of exogenous PTH (1–34) compared with R568 treatment alone. Future studies are needed to delineate the underlying mechanisms.

We next compared osteogenic activity in fracture calluses from mice subjected to daily injections of vehicle, PTH (1–34) (40 μg/kg) alone, or the PTH (1–34)/R568 (20 μmol/kg) combination for 4 weeks. Analyses of hard calluses treated with PTH (1–34) alone by μCT with a 400 mg HA/cm^3 threshold showed a significant increase in Cal.BV/TV (by ≈12% versus vehicle controls, $p < 0.05$) but had no significant effects on Cal.Th or mineral density (Cal.BMD) (Fig. 6B). In contrast, cotreatments with PTH (1–34) and R568 increased Cal.BV/TV by 24% ($p < 0.01$), Cal.Th by 10% ($p < 0.05$) and Cal.BMD by 2.5% ($p < 0.05$) when compared with vehicle controls (Fig. 6B), indicating more robust osteoanabolism than treatment with PTH (1–34) alone. We reasoned that the increased levels of apparent Cal.Th and Cal.BMD might be due to increasing amount of higher-density bone, considering the role of CaSR in promoting mineralizing functions of OBs (Fig. 5). In support of this idea, μCT analyses of calluses treated with combined PTH (1–34)/R568 using a higher threshold for bone mineral density (1000 to 2100 mg HA/ cm^3) showed a larger increase in Cal.BV/TV (by 27% or 13%) and Cal.Th (by 17% or 13%) versus calluses treated with vehicle or PTH (1–34) alone, respectively (Fig. 6C). These data together indicate that the

combined PTH (1–34)/R568 treatment could produce stronger anabolic effects than PTH (1–34) alone in bony calluses without the unwanted calcemic side effects.

Discussion

Our study addresses the role of endogenous CaSRs in chondrogenic and osteogenic cells in the repair of unfixed, long bone fractures in male mice and provides a proof of concept for targeting the CaSR to promote fracture repair. We demonstrate key actions of CaSRs in chondrocytes and OBs in promoting cartilage maturation and bone formation in the early and later stages of bone fracture repair, respectively. We further show a potentiation of callus mineralization and osteogenic activity by dual targeting of the PTH receptor and CaSR, by the combined treatment with PTH (1–34) and R568.

Recent studies using cell lineage tracing techniques uncovered direct chondrocyte transition into the osteoblastic lineage during endochondral bone formation.[8–12] Our observations of the deficient chondrocyte-to-OB transition in GPs and soft calluses lacking chondrocytic CaSRs signify a nonredundant role for this receptor in this cellular transition. Although detailed molecular mechanisms underlying the ability of CaSRs to drive the chondrocyte transition remain to be defined, the reduced IGF1 and IGF1R RNA levels and increased PTHrP gene expression in the soft calluses of the $^{\text{Tam-Cart}}\text{CaSR}^{\Delta\text{flox}/\Delta\text{flox}}$ mice (Fig. 2C) suggest that these two pathways are potential mechanisms interacting with the CaSR. These in vivo CaSR actions in calluses are also compatible with the abilities of raising $[Ca^{2+}]$ and CaSR agonist to promote terminal differentiation, mineralization, and attainment of osteogenic phenotypes in cultures of callus chondrocyte (Fig. 1). Although substantial effort was directed to enrich callus chondrocyte in the culture, we, however, cannot completely rule out a minor inclusion of osteoprogenitors that could contribute to some osteogenic activity in the culture. However, such osteogenic activity is considered minor, as in the cultures grown at 0.5 mM Ca^{2+} for 7 days (a total of 11 days); we observed >90% of the cell areas stained with AG and a 400:1 ratio for the RNA expression of α1(II) over OCN, all indicating a highly enriched chondrocyte culture. Furthermore, the characteristics of our callus chondrocyte culture (growth rate, chondrogenic potential, morphology, and Ca^{2+}-responsiveness) are highly compatible to those of our previous cultures of chondrocytes isolated from the much more homogenous perinatal growth plate cartilage[24,32,33] and a clonal, but not transformed, rat chondrogenic RCJ3.1C5.18 cell line.[25,26] These studies together support the conclusion that the chondro-to-osteo transition is mainly originating from callus chondrocytes per se and not from a population of osteoprogenitors or OB contaminating the chondrocyte preparations.

Our data demonstrate that the CaSR-mediated chondrogenic-to-osteogenic transition is required for a normal progression of repair of unfixed fracture. There is, however, continuous, albeit delayed, progression of fracture repair in bony calluses of $^{\text{Tam-Cart}}\text{CaSR}^{\Delta\text{flox}/\Delta\text{flox}}$ mice, which have drastically reduced numbers of chondrocyte-derived (ie, tdTomato(+)) OB (Fig. 4B), suggesting that the osteogenic activity through recruitment of other osteoprogenitors is also required for fracture repair. Indeed, osteoprogenitors derived from periosteum,[13] muscle,[13–15] pericyte,[16] and bone marrow stromal cells[17–19] have been shown to be critical in mediating the repair of both fixed and

unfixed fractures in animal models. It is unclear whether the CaSR is involved in recruitment or commitment of mesenchymal cells to osteoprogenitors during fracture repair. Nor did our data specify the fate of chondrocyte-derived OBs in the bony calluses after their entry into the OB lineage. Our previous studies of mice with CaSR KO in early OBs (by 2.3 kb-Col(I)-Cre) showed that the CaSR is essential for survival of early OBs.[20] It is therefore likely that the OBs transitioned from chondrocytes could commit to early cell death because of their continuous lack of CaSR expression before acquiring the ability to mediate matrix synthesis and mineralization. Thus, our data from studies of $^{OCN}CaSR^{\Delta flox/\Delta flox}$ mice actually support a role of CaSR in mediating osteogenic activities of mature callus OBs derived from both chondrocytes and other osteoprogenitors. This role of CaSRs in mature OBs is consistent with our previous study demonstrating a nonredundant action of CaSRs in both prenatal and postnatal skeletal development.[20,27]

Our combined PTH (1–34) and R568 regimen overcomes the complications of hyper- or hypocalcemia that can be found, respectively, with each treatment alone and permits development of more robust clinical regimens to treat fracture and perhaps severe osteoporosis by increasing the doses of PTH to achieve more robust osteoanabolism. However, whether these drugs act directly on callus chondrocytes and OBs to produce anabolic synergism remains to be confirmed, despite the fact that their receptors are expressed in those cells. Likewise, how the combined use of PTH (1–34) and R568 normalizes serum Ca^{2+} and Pi levels that are significantly altered by injection of either compound alone remains unclear. These changes in systemic mineral homeostasis likely involve calciotropic actions in other tissues like the parathyroid glands, kidney, intestine, and bone. Future comprehensive studies of tissue-specific ablation of PTH1R and/or CaSR mouse models are needed to gain more insight into those calcemic actions and their synergistic relationship with skeletal anabolism.

Supplementary Material

Refer to Web version on PubMed Central for supplementary material.

Acknowledgments

We thank Drs Daniel Bikle and Robert Nissenson at the San Francisco Department of Veterans Affairs Medical Center and the University of California, San Francisco for critical suggestions during the study. This work was supported by Department of Veterans Affairs Program Project (to DDB, DS, and WC), Merit Review I01BX003453, and Research Career Scientist 1IK6BX004835-01 Awards (to WC); the National Institute of Arthritis and Musculo-skeletal and Skin Diseases (NIAMS) R01-AR067291 and P30-AR066262 (to WC), R01-AR056256 (to CLT), RO1-AR055588 (to DS), and F32DK107177 (to AH).

References

1. National Osteoporosis Foundation. What is Osteoporosis and What Causes It? [Internet]. 9 12, 2019 Available at https://www.nof.org/patients/what-is-osteoporosis/.
2. Bliuc D, Nguyen ND, Nguyen TV, Eisman JA, Center JR. Compound risk of high mortality following osteoporotic fracture and refracture in elderly women and men. J Bone Miner Res. 2013;28(11):2317–24. [PubMed: 23616397]
3. Nakazawa T, Nakajima A, Shiomi K, Moriya H, Einhorn TA, Yamazaki M. Effects of low-dose, intermittent treatment with recombinant human parathyroid hormone (1–34) on chondrogenesis in a model of experimental fracture healing. Bone. 2005;37(5):711–9. [PubMed: 16143574]

4. Tsuchie H, Miyakoshi N, Kasukawa Y, Aonuma H, Shimada Y. Intermittent administration of human parathyroid hormone before osteo-synthesis stimulates cancellous bone union in ovariectomized rats. Tohoku J Exp Med. 2013;229(1):19–28. [PubMed: 23221107]
5. Neer RM, Arnaud CD, Zanchetta JR, et al. Effect of parathyroid hormone (1–34) on fractures and bone mineral density in postmenopausal women with osteoporosis. N Engl J Med. 2001;344(19): 1434–41. [PubMed: 11346808]
6. FDA. NDA#21–318: statistical review and evaluation—clinical studies [Internet]. 9 12, 2019 Available at https://www.accessdata.fda.gov/drugsatfda_docs/nda/2008/021318Orig1s016.pdf.
7. Kronenberg HM. Developmental regulation of the growth plate. Nature. 2003;423(6937):332–6. [PubMed: 12748651]
8. Yang G, Zhu L, Hou N, et al. Osteogenic fate of hypertrophic chondrocytes. Cell Res. 2014;24(10):1266–9. [PubMed: 25145361]
9. Yang L, Tsang KY, Tang HC, Chan D, Cheah KS. Hypertrophic chondrocytes can become osteoblasts and osteocytes in endochondral bone formation. Proc Natl Acad Sci U S A. 2014;111(33):12097–102. [PubMed: 25092332]
10. Zhou X, von der Mark K, Henry S, Norton W, Adams H, de Crombrugghe B. Chondrocytes transdifferentiate into osteoblasts in endochondral bone during development, postnatal growth and fracture healing in mice. PLoS Genet. 2014;10(12):e1004820. [PubMed: 25474590]
11. Hu DP, Ferro F, Yang F, et al. Cartilage to bone transformation during fracture healing is coordinated by the invading vasculature and induction of the core pluripotency genes. Development. 2017;144(2): 221–34. [PubMed: 28096214]
12. Tsang KY, Chan D, Cheah KS. Fate of growth plate hypertrophic chondrocytes: death or lineage extension? Dev Growth Differ. 2015;57(2):179–92. [PubMed: 25714187]
13. Abou-Khalil R, Yang F, Lieu S, et al. Role of muscle stem cells during skeletal regeneration. Stem Cells. 2015;33(5):1501–11. [PubMed: 25594525]
14. Matthews BG, Torreggiani E, Roeder E, Matic I, Grcevic D, Kalajzic I. Osteogenic potential of alpha smooth muscle actin expressing muscle resident progenitor cells. Bone. 2016;84:69–77. [PubMed: 26721734]
15. Matthews BG, Grcevic D, Wang L, et al. Analysis of alphaSMA-labeled progenitor cell commitment identifies notch signaling as an important pathway in fracture healing. J Bone Miner Res. 2014;29(5): 1283–94. [PubMed: 24190076]
16. Supakul S, Yao K, Ochi H, et al. Pericytes as a source of osteogenic cells in bone fracture healing. Int J Mol Sci. 2019;20(5):pii: E1079. [PubMed: 30832329]
17. Park D, Spencer JA, Koh BI, et al. Endogenous bone marrow MSCs are dynamic, fate-restricted participants in bone maintenance and regeneration. Cell Stem Cell. 2012;10(3):259–72. [PubMed: 22385654]
18. Bahney CS, Zondervan RL, Allison P, et al. Cellular biology of fracture healing. J Orthop Res. 2019;37(1):35–50. [PubMed: 30370699]
19. Maes C, Kobayashi T, Selig MK, et al. Osteoblast precursors, but not mature osteoblasts, move into developing and fractured bones along with invading blood vessels. Dev Cell. 2010;19(2):329–44. [PubMed: 20708594]
20. Chang W, Tu C, Chen TH, Bikle D, Shoback D. The extracellular calcium-sensing receptor (CaSR) is a critical modulator of skeletal development. Sci Signal. 2008;1(35):ra1. [PubMed: 18765830]
21. Santa Maria C, Cheng Z, Li A, et al. Interplay between CaSR and PTH1R signaling in skeletal development and osteoanabolism. Semin Cell Dev Biol. 2016;49:11–23. [PubMed: 26688334]
22. Hannan FM, Kallay E, Chang W, Brandi ML, Thakker RV. The calcium-sensing receptor in physiology and in calcitropic and noncalcitropic diseases. Nat Rev Endocrinol. 2018;15(1):33–51. [PubMed: 30443043]
23. Chang W, Tu C, Chen TH, et al. Expression and signal transduction of calcium-sensing receptors in cartilage and bone. Endocrinology. 1999;140(12):5883–93. [PubMed: 10579354]
24. Rodriguez L, Cheng Z, Chen TH, Tu C, Chang W. Extracellular calcium and parathyroid hormone-related peptide signaling modulate the pace of growth plate chondrocyte differentiation. Endocrinology. 2005;146(11):4597–608. [PubMed: 16099862]

25. Chang W, Tu C, Bajra R, et al. Calcium sensing in cultured chondrogenic RCJ3.1C5.18 cells. Endocrinology. 1999;140(4):1911–9. [PubMed: 10098531]
26. Chang W, Tu C, Pratt S, Chen TH, Shoback D. Extracellular Ca(2+)-sensing receptors modulate matrix production and mineralization in chondrogenic RCJ3.1C5.18 cells. Endocrinology. 2002;143(4): 1467–74. [PubMed: 11897705]
27. Dvorak-Ewell MM, Chen TH, Liang N, et al. Osteoblast extracellular Ca2+-sensing receptor regulates bone development, mineralization, and turnover. J Bone Miner Res. 2011;26(12):2935–47. [PubMed: 21956637]
28. Nakamura E, Nguyen MT, Mackem S. Kinetics of tamoxifen-regulated Cre activity in mice using a cartilage-specific CreER(T) to assay temporal activity windows along the proximodistal limb skeleton. Dev Dyn. 2006;235(9):2603–12. [PubMed: 16894608]
29. Madisen L, Zwingman TA, Sunkin SM, et al. A robust and high-throughput Cre reporting and characterization system for the whole mouse brain. Nat Neurosci. 2010;13(1):133–40. [PubMed: 20023653]
30. Zhang M, Xuan S, Bouxsein ML, et al. Osteoblast-specific knockout of the insulin-like growth factor (IGF) receptor gene reveals an essential role of IGF signaling in bone matrix mineralization. J Biol Chem. 2002; 277(46):44005–12. [PubMed: 12215457]
31. Wang T, Wang Y, Menendez A, et al. Osteoblast-specific loss of IGF1R signaling results in impaired endochondral bone formation during fracture healing. J Bone Miner Res. 2015;30(9):1572–84. [PubMed: 25801198]
32. Rodriguez L, Tu C, Cheng Z, et al. Expression and functional assessment of an alternatively spliced extracellular Ca2+-sensing receptor in growth plate chondrocytes. Endocrinology. 2005;146(12): 5294–303. [PubMed: 16166224]
33. Cheng Z, Tu C, Rodriguez L, et al. Type B gamma-aminobutyric acid receptors modulate the function of the extracellular Ca2+-sensing receptor and cell differentiation in murine growth plate chondrocytes. Endocrinology. 2007;148(10):4984–92. [PubMed: 17615148]
34. Cheng Z, Liang N, Chen TH, et al. Sex and age modify biochemical and skeletal manifestations of chronic hyperparathyroidism by altering target organ responses to Ca2+ and parathyroid hormone in mice. J Bone Miner Res. 2013;28(5):1087–100. [PubMed: 23239173]
35. Dempster DW, Compston JE, Drezner MK, et al. Standardized nomenclature, symbols, and units for bone histomorphometry: a 2012 update of the report of the ASBMR Histomorphometry Nomenclature Committee. J Bone Miner Res. 2013;28(1):2–17. [PubMed: 23197339]
36. Chang W, Pratt S, Chen TH, Nemeth E, Huang Z, Shoback D. Coupling of calcium receptors to inositol phosphate and cyclic AMP generation in mammalian cells and Xenopus laevis oocytes and immunodetection of receptor protein by region-specific antipeptide antisera. J Bone Miner Res. 1998;13(4):570–80. [PubMed: 9556057]
37. Nemeth EF, Heaton WH, Miller M, et al. Pharmacodynamics of the type II calcimimetic compound cinacalcet HCl. J Pharmacol Exp Ther. 2004;308(2):627–35. [PubMed: 14593085]

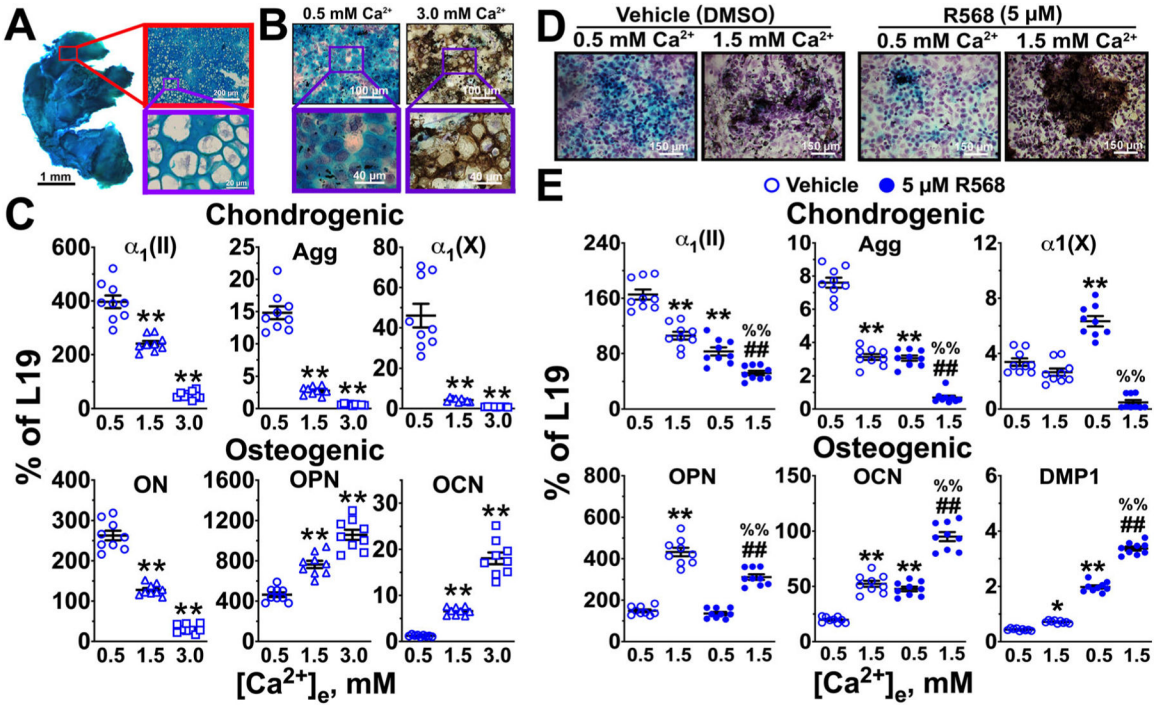

Fig. 1.

Chondrogenic and osteogenic responses of callus chondrocytes to changes in $[Ca^{2+}]_e$ and CaSR agonist. Cartilage and chondrocyte cultures were prepared from calluses of C57/B6 mice 10 days after fracture. (*A*) Left panel: A representative micro-dissected cartilage, co-stained with Alcian green (AG) and alizarin red (AR), shows enriched cartilaginous elements deprived of surrounding bone tissue (lack of AR staining). Right panels: Sections of micro-dissected callus cartilage, co-stained with AG, AR, and hematoxylin, also confirm the absence of AR-positive bone tissue. Scale bar = 1 mm. (*B*) AG and von Kossa (VK) staining and (*C*) RNA expression of chondrogenic (aggrecan and α_1 subunits of type II [α_1(II)] and type X [α_1(X)] collagen) and osteogenic (osteonectin [ON], osteopontin [OPN] and osteocalcin [OCN]) markers in callus chondrocytes cultured at different $[Ca^{2+}]_e$ for 7 days. These experiments show the ability of raising $[Ca^{2+}]_e$ (from 0.5 to 3.0 mM) to reduce AG staining and expression of chondrogenic markers and to increase VK staining and the expression of osteogenic markers. RNA levels were normalized to ribosomal L_{19} expression, mean ± SEM, $n = 3$ batches (in triplicate) of chondrocytes isolated from 30 calluses; $^{**}p <$ 0.01 versus 0.5 mM Ca^{2+} by one-way ANOVA with Tukey's test for multiple comparisons. (*D*) AG and VK staining and (*E*) gene expression in callus chondrocytes cultured in 0.5 and 1.5 mM Ca^{2+} with vehicle (DMSO) or 5 μM R568 for 7 days show the ability of R568 to potentiate the effects of $[Ca^{2+}]_e$, mean ± SEM, $n = 3$ batches (in triplicate) of chondrocytes isolated from 30 calluses; $^{**}p < 0.01$ versus 0.5 Ca^{2+}/vehicle; $^{\#\#}p < 0.01$ versus 0.5 Ca^{2+}/R568; $^{\%\%}p < 0.01$ versus 1.5 Ca^{2+}/vehicle; two-way ANOVA with Tukey's test for multiple comparisons.

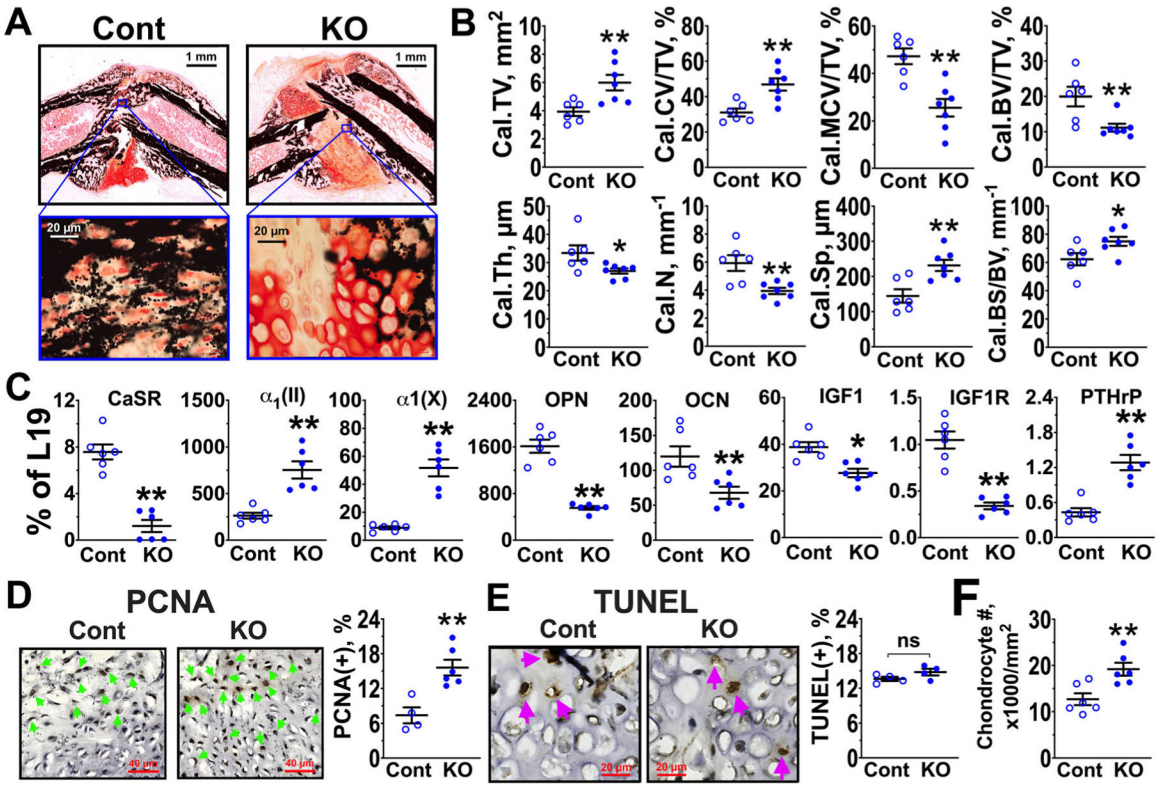

Fig. 2.

Ablation of CaSRs promotes chondrocyte proliferation and delays maturation and transition of cartilage to bone in soft calluses at day 10 post-fracture. (*A*) Representative images and (*B*) histomorphometric quantifications of Safranin O (SO) and VK-stained callus sections from 3-month-old male $^{\text{Tam-Cart}}\text{CaSR}^{\Delta\text{flox}/\Delta\text{flox}}$ (KO) and control (Cont) littermates. VK reagent stains mineralized matrix (in black), and SO reagent stains proteoglycan-rich cartilage (in red). Total callus volume (Cal.TV), callus cartilage fraction (Cal.CV/TV), callus mineralized cartilage over Cal.CV ratio (Cal.MCV/CV), and callus bone fraction (Cal.BV/TV), thickness (Cal.Th), number (Cal.N), spacing (Cal.Sp), and surface/volume ratio (Cal.BS/BV) were measured. Mean ± SEM, $n = 6$ (Cont) and 7 (KO) mice; $^{*}p < 0.05$, $^{**}p < 0.01$ versus Cont, Student's *t* test. (*C*) qPCR analyses of RNA extracted from calluses, excluding preexisting cortical bone fragments, show profound reductions in CaSR RNA expression along with increased expression of chondrogenic markers [α_1(II) and α_1(X)], reduced expression of osteogenic markers (OPN and OCN), increased insulin-like growth factor 1 (IGF1) and receptor (IGF1R) expression, and increased PTH-related peptide (PTHrP) expression in the KO versus Cont mice. RNA levels were normalized to L_{19}. Mean ± SEM; $n = 2$ batches of RNA (in triplicate) from a total of 24 (Cont) and 20 (KO) mice/group; $^{*}p < 0.05$, $^{**}p < 0.01$ versus Cont, Student's *t* test. (*D*–*F*) Representative images of the (*D*) PCNA-stained or (*E*) TUNEL-stained chondrocytes and their quantifications in callus of $^{\text{Tam-Cart}}\text{CaSR}^{\Delta\text{flox}/\Delta\text{flox}}$ (KO) and control (Cont) littermates at day 10 post-fracture. PCNA (green arrowheads) or TUNEL (pink arrowheads) immunoreactivity, indicated by brown DAB stain, was co-stained with hematoxylin (purplish blue). Scatter plots show the numbers of (*D*) PCNA(+) or (*E*) TUNEL(+) cells normalized to total hematoxylin(+) cell

numbers or (*F*) total number of hematoxylin(+) cells per mm^2 to indicate cellular density in the callus cartilage. Mean ± SEM; $n = 4$ Cont and 6 KO mice/group; $^{**}p < 0.01$ versus Cont, Student's *t* test.

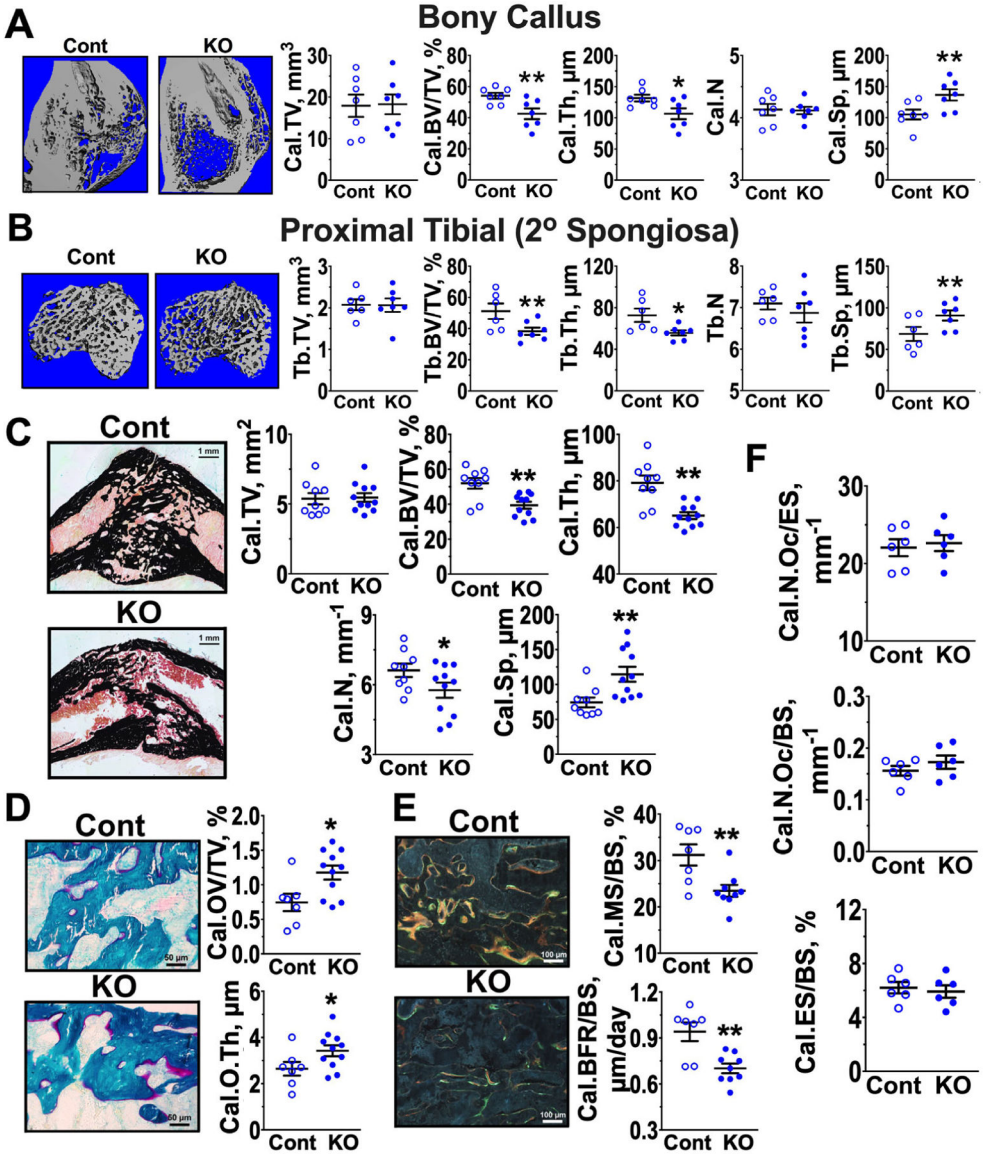

Fig. 3.

Ablation of chondrocyte CaSR retards osteogenesis and impairs mineralizing function in tibial secondary spongiosa and/or bony calluses. μCT and histomorphometric analyses and their quantifications were performed on bony calluses and/or tibial secondary spongiosa from 3-month-old male $^{\text{Tam-Cart}}\text{CaSR}^{\Delta\text{flox}/\Delta\text{flox}}$ (KO) and control (Cont) littermates at day 28 post-fracture. (*A*, *B*) μCT images and quantifications revealed osteopenic calluses and secondary spongiosa of proximal tibias of contralateral (unfractured) bone as indicated by reduced Tb.BV/TV, Cal.BV/TV, Tb.Th, Cal.Th, and increased Cal.Sp and Tb.Sp in the KO versus Cont mice. Mean ± SEM, $n = 7$ mice/group; $^{*}p < 0.05$, $^{**}p < 0.01$ versus Cont, Student's *t* test. (*C*, *D*) Static histomorphometry using VK and SO staining confirmed thinner bony calluses (*C*), whereas Goldner staining shows larger amounts of unmineralized osteoid (in pink) on the bone surface (*D*) in the calluses of KO versus Cont mice, indicating defective mineralizing functions of OBs. Cal.OV/TV = callus osteoid volume/TV; Cal.O.Th

= callus osteoid thickness. Mean ± SEM, $n = 9$ Cont and 11 KO mice; *$p < 0.05$, **$p < 0.01$ versus Cont, Student's t test. (*E*) Dynamic bone parameters—callus mineralizing surface/BS ratio (Cal.MS/BS) and bone formation rate/BS ratio (Cal.BFR/BS)—as assessed by sequential dual demeclocycline (orange) and calcein (in green) labeling further confirmed defective mineralizing function of callus OBs in KO versus Cont mice. Mean ± SEM, $n = 9$ Cont and 11 KO mice; *$p < 0.05$, **$p < 0.01$ versus Cont, Student's t test. (*F*) Static histomorphometry using TRAP staining showed unchanged osteoclastogenic activities as indicated by Cal.N.Oc/ES (number of callus osteoclasts/erosion surface), Cal.N.Oc/BS (number of callus osteoclasts/bone surface), or Cal.ES/BS (percentage of callus erosion surface/bone surface). Mean ± SEM, $n = 6$ Cont and 6 KO mice.

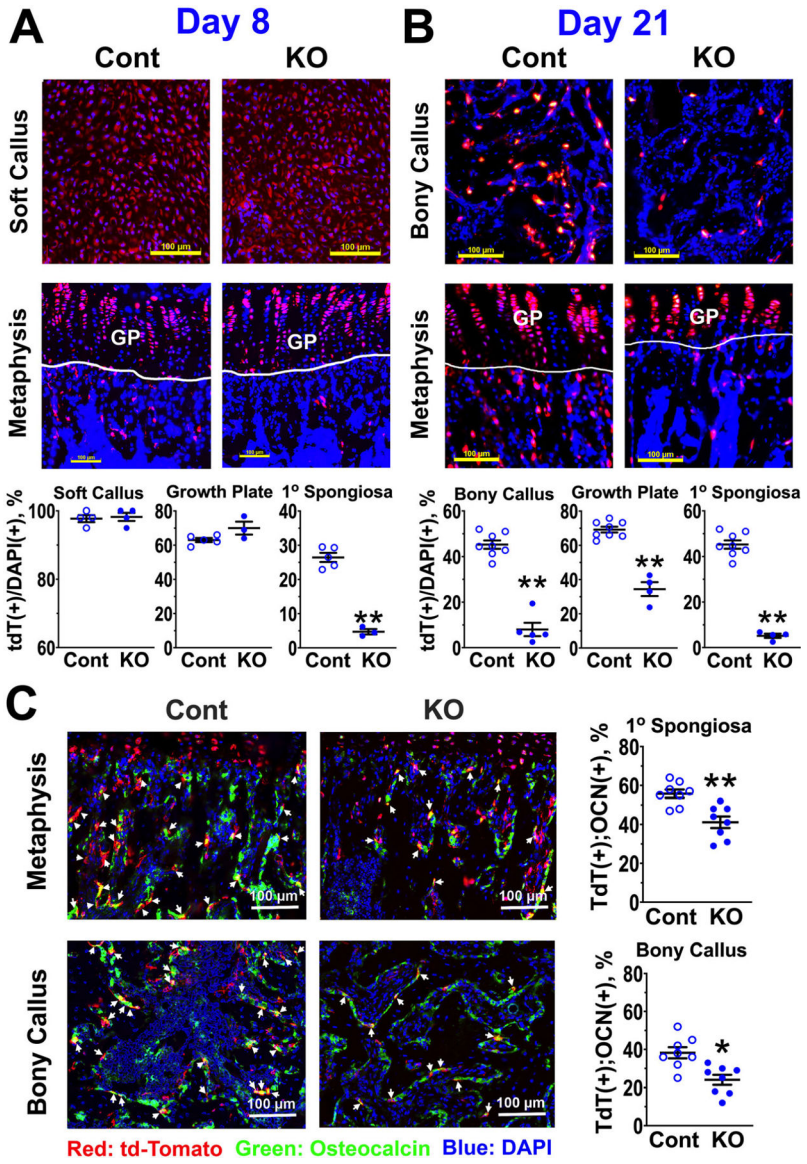

Fig. 4.

Reduced transition of callus chondrocyte into osteoblast in calluses of CaSR KO versus control mice. Labeling of cell with tdTomato red fluorescent protein was performed in the background of $^{\text{Tam-Cart}}\text{CaSR}^{\Delta\text{flox}/\Delta\text{flox}}$ (KO) and control (Cont) littermates by 9 daily tam injections, starting 1 day before bone fracture. (*A*) Sections of soft callus and metaphysis stained with blue fluorescent DAPI show comparable numbers of tdTomato(+) callus chondrocytes as well as tdTomato(+) GP chondrocytes between Cont and KO groups. However, the numbers of tdTomato(+) OB in the spongiosa were significantly reduced in the KO versus Cont group. Numbers of tdTomato(+) chondrocytes were normalized and presented as % of total DAPI(+) cells in the regions of interest. Mean ± SEM, $n = 6$ Cont and 8 KO mice/group; $^{**}p < 0.01$ versus Cont, Student's t test. (*B*) Similarly, decreased tdTomato(+) OB numbers in bony calluses and spongiosa of KO versus Cont mice were found at day 21 post-fracture along with decreased numbers of tdTomato(+) chondrocytes in

their GPs. Mean ± SEM, $n = 9$ Cont and 6 KO mice/group; $^{**}p < 0.01$ versus Cont, Student's t test. (*C*) Representative images of immunohistochemical localization of OB marker, OCN to tdTomato(+) OBs (white arrowheads) in spongiosa and bony calluses of $^{\text{Tam-Cart}}\text{CaSR}^{\Delta\text{flox}/\Delta\text{flox}}$ (KO) and control (Cont) mice. Scatter plots show % of cells, which were stained positively for both tdTomato and OCN, after normalized to the number of total tdTomato(+) cell in 1° and 2° spongiosa or bony callus at day 21 post-fracture. Mean ± SEM, $n = 8$ Cont and 8 KO mice/group; $^{**}p < 0.01$, $^{*}p < 0.05$ versus Cont, Student's t test.

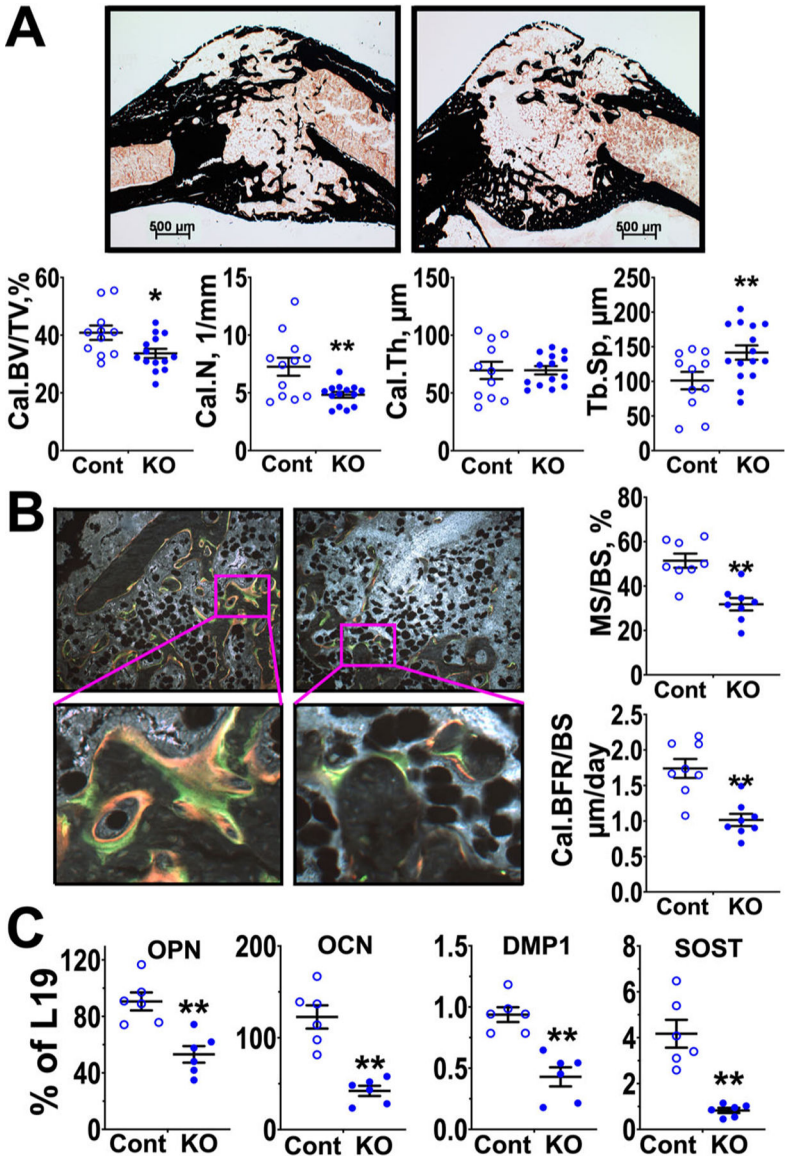

Fig. 5.

Ablation of CaSRs in mature OBs retards osteogenesis and impairs mineralizing function in bony calluses. Histomorphometric and RNA analyses were performed on bony calluses of 3-month-old male $^{OCN}CaSR^{\Delta flox/\Delta flox}$ (KO) and control (Cont) littermates at day 28 post-fracture. (*A*) Static histomorphometry using VK and SO staining shows reduced Cal.BV/TV, Cal.N, and Cal.Th, and increased Cal.Sp, in the calluses of KO versus Cont mice. Mean ± SEM, $n = 14$ KO and 11 Cont mice/group; $^{*}p < 0.05$, $^{**}p < 0.01$ versus Cont, Student's *t* test. (*B*) Dynamic bone parameters (Cal.MS/BS and Cal.BFR/BS) show defected mineralizing function in KO versus Cont mice. Mean ± SEM, $n = 8$ KO and 8 Cont mice; $^{**}p < 0.01$ versus Cont, Student's *t* test. (*C*) qPCR analyses of RNA extracted from calluses, excluding preexisting cortical bone fragments, show profound reductions in osteogenic markers in the KO versus Cont mice. RNA levels were normalized to L_{19}. Mean ± SEM, $n =$

3 batches (in duplicate) of RNA from a total of 9 (Cont) and 10 (KO) mice/group; *$p < 0.05$, **$p < 0.01$ versus Cont, Student's *t* test.

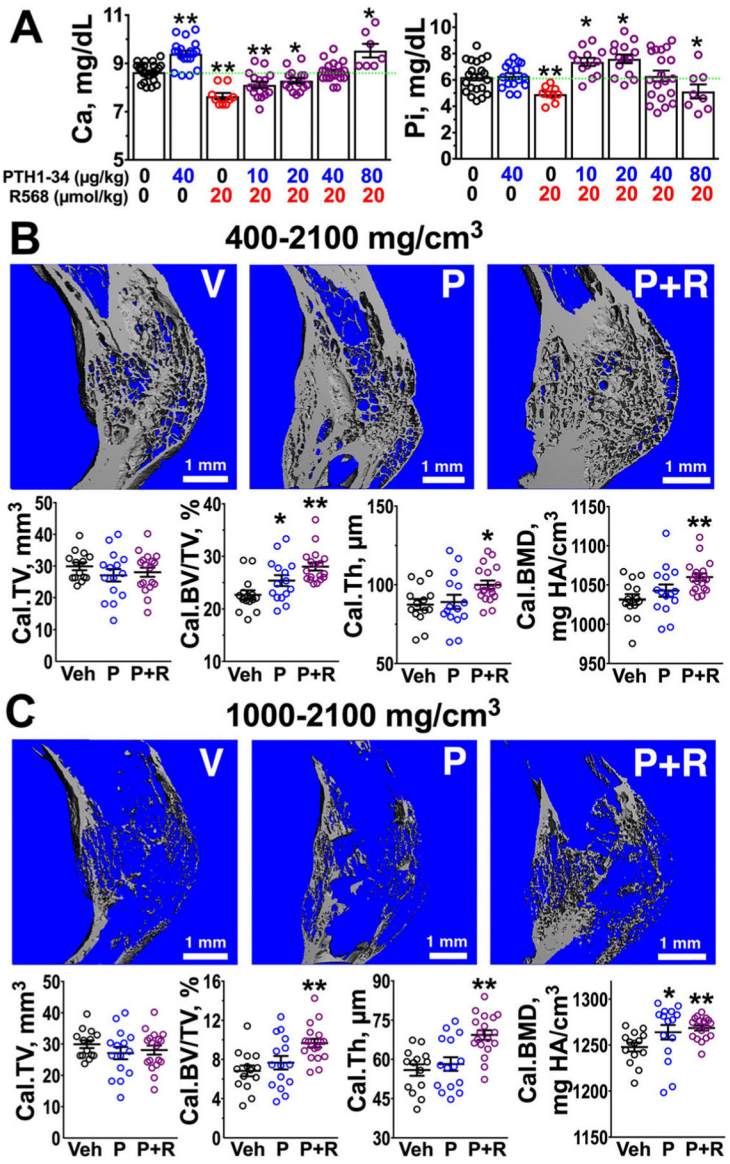

Fig. 6.

Co-injections of calcimimetic NPS-R568 offset hypercalcemic side effects of PTH (1–34) and produce synergistic osteoanabolism in bony calluses. Serum Ca^{2+} and phosphate (Pi) levels and μCT analyses of bony calluses in 3-month-old male C57/B6 male mice subjected to tibial fracture and daily injections of vehicle (V), PTH (1–34) (P, 40 μg/kg B.Wt.), or PTH (1–34)+R568 (P + R, 20 μmol/kg B.Wt) for 28 days. (*A*) Serum Ca^{2+} and Pi levels, determined by clinical bioanalyzers, show the ability of R568 to offset hypercalcemic effects of PTH (1–34) in a dose-dependent manner. (*B, C*) 3D μCT images and their structural parameters (histograms) assessed with (*B*) 400–2100 mg HA/cm^3 or (*C*) 1000–2100 mg HA/cm^3 thresholds, which measure total and high-density bone, respectively, show the synergistic effects of R568 to increase osteoanabolism of PTH (1–34). Mean ± SEM, n = 15–17 mice/group; *$p < 0.05$; **$p < 0.01$ versus vehicle, two-way ANOVA with Tukey's test for multiple comparisons.